Available online at www.sciencedirect.com
ScienceDirect
Ceramics International 37 (2011) 2727–2735
CERAMICS INTERNATIONAL
www.elsevier.com/locate/ceramint

Mechanical properties of flame sprayed free-standing coatings

T. Kratschmer *, C.G. Aneziris, P. Gruner

Institute of Ceramics, Glass and Construction Materials, TU BA Freiberg, Germany

Received 11 February 2011; received in revised form 12 April 2011; accepted 14 April 2011
Available online 23 April 2011

Abstract

This paper examines the mechanical properties of rod flame sprayed coatings in the system Al_2O_3–TiO_2–ZrO_2. Free-standing thin coatings were tested and a new approach for their preparation was used and assessed in terms of absolute values of bending strength and their standard deviation in comparison with published values for ceramic systems. The Young's modulus shows distinct non-linear behavior. The presence of particle-, micro crack- and/or transformation toughening mechanisms can be seen by comparing mechanical properties of pure alumina- with zirconia containing coatings.

Keywords: C. Mechanical properties; Thermal spray; Thermo shock; Alumina; Titania; Zirconia

1. Introduction

Determination of mechanical properties of thermally sprayed materials has been a widely aimed goal. A common way hereby is to spray thick layers and cut specimens from that block or cylinder [1–11]. Another frequently used strategy to obtain characteristic values for bending strength, adhesion strength, Young's modulus, fracture strain, number of survived thermal shock cycles etc. is testing the composite, i.e. coating with substrate [12–34] and the application of indentation methods [15,19,23–25,27,28,35–51]. Hereby the non-trivial interaction between substrate and coating has to be taken into account. The number of publications applying indentation method shows, that this method is very popular due to its low sample preparation complexity. The cutting and polishing procedure influences the micro crack network in an undetermined way. To minimize this impact of forces to the specimen prior testing some authors follow the strategy of spraying samples on thermally or chemically removable substrates [2–4,7,52,53]. The dimensions of the coated and later removed substrate represent the final dimensions of the free-standing coating. With this technique it is possible to produce free standing stripes with thicknesses in the range of 0.6 to several mm [4,7,52,53] that are suitable for 3- or 4-point bending experiments. The Young's modulus of thermally sprayed materials shows typically non-linear behavior [13,33,54–56].

This paper describes a new approach of producing thin stripes of ceramic coatings for mechanical property determination and even for thermal shock experiments. The new approach is that the coating is built up on a substrate with adjusted roughness that on the one hand provides enough adhesion for coating built up but on the other hand enables the removal of the coating after the spray process with nearly no applied force. The substrate is additionally covered with a template for producing stripes of the coating in the dimensions 10 mm width and up to 100 mm length. The results of the so tested ceramic composites were compared with a compilation (Table 1) of published mechanical properties for several thermally sprayed oxide materials. There is a large scatter for mechanical properties found in literature. The big influence of spray parameters and different spray process explains most of that scatter. For oxide systems the bending strength normally lies in the range between 20 and 80 MPa; peak values for the alumina–zirconia system of 160 MPa can be found. If the values are much lower, very likely non-optimum spray parameters were applied. Most data are published for alumia- and stabilized zirconia-matrix systems. After a heat treatment the bending strength and the Young's modulus normally show strong increase due to sintering and densification. If processes appear that lead to the formation of cracks, the mechanical cohesion

* Corresponding author.
E-mail address: tim.kratschmer@gmail.com (T. Kratschmer).

0272-8842/$36.00
doi:10.1016/j.ceramint.2011.04.027

Table 1
Compiled mechanical properties of thermally sprayed oxides.

Material (type, sample treatment, etc.)	Process	Bending strength σ [MPa]	Young's modulus [Gpa]	Fracture strain ε [%]	Fracture toughness K_{IC} [MPa $m^{1/2}$]	Porosity [%]	Roughness [μm]	Weibull modulus [–]	Type of test, comments	Ref.
Al_2O_3-matrix										
Al_2O_3	APS	20	–	–	1.2	–	–	–	4-Point-bending, in situ observation of crack extension via REM	[9]
Al_2O_3 (12 h/1550 °C)	APS	60	–	–	5	–	–	–	4-Point-bending, in situ observation of crack extension via REM	[9]
Al_2O_3	RFS	~35	~45	–	–	7.6	–	–	3-Point-bending of free-standing samples	[57]
Al_2O_3	APS	27.2 ± 1.7	13	–	–	–	–	–	Ring-test	[11]
Al_2O_3 (4 h/1450 °C)	APS	54.8 ± 4.1	95	–	–	–	–	–	Ring-test	[11]
Al_2O_3	LPPS	120	70	–	–	–	–	26 (0.3 mm) 37 (0.7 mm)	4-Point-bending with aluminium substrate; layer thickness 0.3 and 0.7 mm	[58]
Al_2O_3/3 wt%TiO_2	APS	35.6 ± 2.7	17	–	–	–	–	–	Ring-test	[11]
Al_2O_3/3 wt%TiO_2 (4 h/1450 °C)	APS	125 ± 27	260	–	–	–	–	–	Ring-test	[11]
Al_2O_3/13 wt%TiO_2 (Metco 130SF)	APS	17.6	14.0	1.7*	–	–	4.3 (Ra)	–	3-Point-bending of free-standing impregnated samples; indentation method (Vickers); *fracture strain very likely in ‰	[7]
Al_2O_3/13 wt%TiO_2 (Metco 130SF, Metcoseal URS)	APS	14.6	13.6	1.5*	–	–	0.3 (Ra)	–	3-Point-bending of free-standing impregnated samples; indentation method (Vickers); *fracture strain very likely in ‰	[7]
Al_2O_3/13 wt%TiO_2 (Metco 130SF, Metcoseal ERS)	APS	11.4	13.5	1.1*	–	–	0.3 (Ra)	–	3-Point-bending of free-standing impregnated samples; indentation method (Vickers); *fracture strain very likely in ‰	[7]
Al_2O_3/13 wt%TiO_2 (Metco 130SF, Dichtol)	APS	12.8	12.4	1.3*	–	–	0.3 (Ra)	–	3-Point-bending of free-standing impregnated samples; indentation method (Vickers); *fracture strain very likely in ‰	[7]
Al_2O_3/50 wt%TiO_2	APS	31	236	–	–	6	5.28	–	Indentation method (Vickers, Knoop); 3-point-bending of layer and substrate	[23]
Al_2O_3/50 wt%TiO_2 (16 h/600 °C)	APS	13.2	–	–	–	8	–	–	indentation method (Vickers, Knoop); 3-point-bending of layer and substrate	[23]
Al_2O_3/30 wt%MgO	APS	103	10	2.3*	–	6.1	–	–	3-Point-bending of free-standing samples; *fracture strain very likely in ‰	[54]
Al_2O_3/22.3 wt%ZrO_2	APS	32.8 ± 1.7	20	–	–	–	–	–	Ring-test	[11]
Al_2O_3/22.3 wt%ZrO_2 (4 h/1450 °C)	APS	76.0 ± 4.6	95	–	–	–	–	–	Ring-test	[11]
Al_2O_3/40 wt%ZrO_2	APS	81	8.8	1.6*	–	5.9	–	–	3-Point-bending of free-standing samples; *fracture strain very likely in ‰	[54]
Al_2O_3/40 wt%ZrO_2	APS	163 ± 26	150 ± 22	0.13 ± 0.01	–	12.3 ± 0.6	–	6	3-Point-bending of free-standing samples	[1]
Al_2O_3/40 wt%ZrO_2 (1 h/1400 °C)	APS	156 ± 17	160 ± 41	0.15 ± 0.02	–	7.9 ± 0.4	–	3	3-Point-bending of free-standing samples	[1]

ZrO_2-matrix										
ZrO_2/7 wt%Y_2O_3	APS	74	21.3	0.8*	–	12	–	–	3-Point-bending of free-standing samples; *fracture strain very likely in ‰	[54]
ZrO_2/7 wt%Y_2O_3	APS	74	16	–	–	11.9	–	25	3-Point-bending of free-standing samples	[10]
ZrO_2/7 wt%Y_2O_3 (48 h/1000 °C)	APS	123	31	–	–	10.9	–	18	3-Point-bending of free-standing samples	[10]
ZrO_2/7 wt%Y_2O_3 (48 h/1000 °C + 36 h/ 1400 °C)	APS	314	45	–	–	8.7	–	20	3-Point-bending of free-standing samples	[10]
ZrO_2/7 wt%Y_2O_3 (48 h/1000 °C + 24 h/ 1700 °C)	APS	10	4	–	–	12.8	–	5	3-Point-bending of free-standing samples	[10]
ZrO_2/7 wt%Y_2O_3	APS	~115	~55	–	–	11	–	-	4-Point-bending of free-standing samples	[4]
ZrO_2/7 wt%Y_2O_3 (1000 h/1250 °C)	APS	~180	~105	–	–	–	–	-	4-Point-bending of free-standing samples	[4]
ZrO_2/8 wt%Y_2O_3	APS	~55	~35	–	–	15	–	-	4-Point-bending of free-standing samples	[4]
ZrO_2/8 wt%Y_2O_3 (1000 h/1250 °C)	APS	~85	~55	–	–	–	–	-	4-Point-bending of free-standing samples	[4]
ZrO_2/8 wt%Y_2O_3	APS	33 ± 7	13 (tension) 25 (compression)	–	KIc: 1.15 ± 0.07 KIIc: 0.73 ± 0.10	–	–	6	4-Point-bending of free-standing samples, SEVNB	[5]
ZrO_2/8 wt%Y_2O_3	APS	39.7 ± 2.7	9.9 ± 0.6	–	–	–	–	–	4-Point-bending of free-standing samples	[52]
ZrO_2/8 wt%Y_2O_3 (5 h/1250 °C)	APS	91.3 ± 3.9	40.9 ± 4.1	–	–	–	–	–	4-Point-bending of free-standing samples	[52]
ZrO_2/8 wt%Y_2O_3 (laser treated)	APS	10.8 ± 2.1	1–3	–	–	–	–	–	4-Point-bending of free-standing samples	[52]
ZrO_2/8 wt%Y_2O_3 (laser treated. 5 h/ 1250 °C)	APS	19.1 ± 1.4	5–8	–	–	–	–	–	4-Point-bending of free-standing samples	[52]
ZrO_2/8 wt% Y_2O_3 (Amperit 827.090, tested at RT, 500 °C and 1000 °C)	APS	4–60	2.5–20	0.2–0.4	–	–	–	–	Free-standing samples	[33]
ZrO_2/(xY_2O_3;$yCeO_2$) (0–1000 h/ 1000–1400 °C)	APS	10–65	10–90	–	–	–		–	4-Point-bending of free-standing samples	[53]
Ca-ZrO_2	APS	25.3 ± 3.1	7	–	–	–	–	–	Ring-test	[11]
Ca-ZrO_2 (4 h/1450 °C)	APS	78.2 ± 9.9	106	–	–	–	–	–	Ring-test	[11]
Mg-ZrO_2	APS	13.9 ± 0.2	3.7	–	–	–	–	–	Ring-test	[11]
Mg-ZrO_2 (4 h/1450 °C)	APS	50.1 ± 2.0	69	–	–	–	–	–	ring-test	[11]
Other oxides										
HA	HVOF	41.4 ± 3.9	–	–	–	–	4.7 (Ra)	–	4-Point-bending of free-standing samples	[31]
HA	APS	45.2 ± 5.1	–	–	–	–	3.1 (Ra)	–	4-Point-bending of free-standing samples	[31]
HA	APS	6–14	0.5–3.4 (tension) 3.2–5.3 (compression)	–	0.3–1.1	–	6–8 (Ra)	–	Bending of layer with substrate	[32]
$La_2Ce_2O_7$	APS	20.3	25	–	1.3–1.5	–	–	–	Indentation method (Vickers, Knoop)	[36]
$MgAl_2O_4$	APS	26.7 ± 2.8	16	–	–	–	–	–	Ring-test	[11]
$MgAl_2O_4$ (4 h/1450 °C)	APS	64.3 ± 4.7	119	–	–	–	–	–	Ring-test	[11]
Mullite	APS	28.6 ± 2.1	16	–	–	–	–	–	Ring-test	[11]
Mullite (4 h/1450 °C)	APS	37.7 ± 5.6	46	–	–	–	–	–	Ring-test	[11]
$ZrSiO_4$	APS	19.3 ± 2.1	6.1	–	–	–	–	–	Ring-test	[11]
$ZrSiO_4$ (4 h/1450 °C)	APS	Fail	–	–	–	–	–	–	Ring-test	[11]

APS = atmospheric plasma spraying; RFS = rod flame spraying; LPPS = low pressure plasma spraying; HVOF = high velocity oxy-fuel flame spraying; HA = hydroxyapatite.

Table 2
Sample composition and denomination.

Sample denomination	Al_2O_3 [wt%]	TiO_2 [wt%]	ZrO_2 [wt%]
100:0:0	100	0	0
90:0:10	90	0	10
90:10:0	90	10	0
90:5:5	90	5	5
85:5:10	85	5	10
85:10:5	85	10	5
80:10:10	80	10	10

can completely disappear. The standard deviations given in some publications are in the range of 5–15% of the according property.

2. Materials and methods

Samples were prepared using the method of substrate with adjusted roughness; the roughness was hereby at Ra = 2 μm and Rz = 15 μm. For a good adhesion of thermally sprayed coatings the substrate roughness should be one order of magnitude higher [59]. The thickness of the produced samples was adjusted to 0.5 mm. Seven different compositions were tested, sample composition and denomination are given in Table 2. All compositions were tested as sprayed and after heat treatment. The heat treatment with different time and temperature combinations is specified in Table 3. The treatment temperature of 1200 °C was chosen in a way that the phase change from γ- to α-Al_2O_3 should thermodynamically be completed, the different times of 10 and 100 h were chosen to evaluate the kinetics of this transformation in dependence of the composition. The highest treatment temperature of 1600 °C was taken from the maximum application temperature for pure alumina. In the style of a statistical experimental set up also the center point of this matrix was included as treatment stage. For heat treatment the samples were covered with coarse corundum. Bending strength, fracture strain and Young's modulus were calculated from 3-point-bending experiments. The rod production, spray parameters, raw materials and experimental set ups are described elsewhere [60–63].

3. Results and discussion

All data of mechanical properties are summarized in Table 4. Their discussion will follow in the next sections. Due to the non-elastic behavior the Young's moduli are given at relative strain levels of 0.2 and 0.8, the ratio of the two values indicate the degree of non-linearity. Additionally the later defined type or character of the instantaneous modulus was determined for every tested sample. There is no standard deviation given for the Young's moduli, their scatter lies in the range of ±20%.

Table 3
Sample heat treatment.

Temperature/time	1200 °C	1400 °C	1600 °C
10 h	x		x
55 h		x	
100 h	x		x

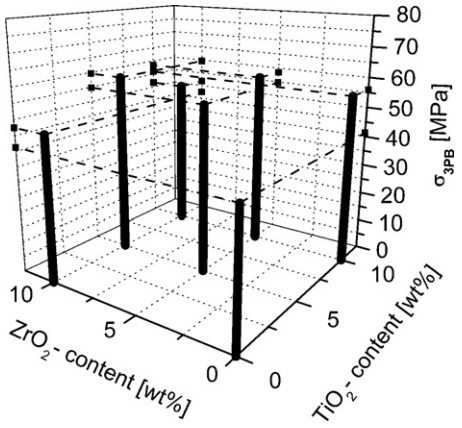

Fig. 1. Bending strength as sprayed.

3.1. Bending strength and fracture strain

There is Ref. [57] presenting data about rod flame sprayed alumina and this value matches the current finding pretty well. Also the measured values of all other compositions lie in the range of the compiled mechanical properties and show a comparable standard deviation. Thus the presented method of preparing and testing thin free standing coatings is suitable for material characterization.

In the as sprayed state the bending strength (Fig. 1) increases starting from pure alumina with increasing amount of additions up to 15 wt% additions. This maximum in strength may correspond with the standard composition of the commercial available and widely used mixture Al_2O_3/13 wt% TiO_2. The fracture strain decreases with increasing amount of addition. Both tendencies can be explained with the increasing amount of amorphous content (see Ref. [63]) that leads to a better cohesion between both the lamellae and the columnar grown crystals within the lamellae with the secondary amorphous zones having higher influence on strength.

The heat treatment causes two different effects: sintering and growth of precipitated phases. The first process increases the bending strength and decreases the fracture strain remarkably.

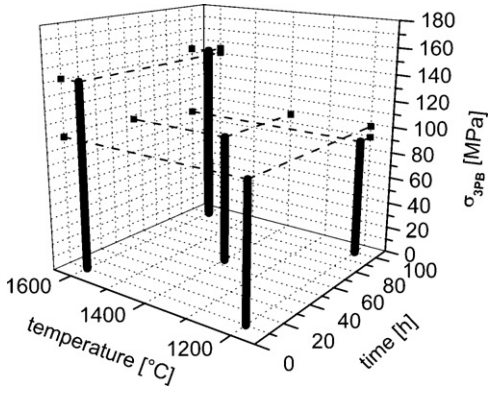

Fig. 2. Strength evolution of 100:0:0.

Table 4
Mechanical properties.

Sample	Treatment	Bending strength σ [MPa]	Fracture strain ε [‰]	Young's modulus		Type of instantaneous modulus
				$E_{0.2}$ [GPa]	$E_{0.8}$ [GPa]	
100:0:0	as sprayed	41.3 ± 2.8	2.30 ± 0.20	20	18	1–2
	10 h 1200 °C	98.0 ± 8.0	1.28 ± 0.18	73	73	2
	100 h 1200 °C	89.3 ± 14.1	1.22 ± 0.13	73	71	2
	55 h 1400 °C	96.8 ± 10.1	0.90 ± 0.10	112	118	2–3
	10 h 1600 °C	140.6 ± 20.8	0.99 ± 0.16	118	130	3
	100 h 1600 °C	144.1 ± 24.6	0.83 ± 0.09	147	170	3
90:0:10	as sprayed	47.5 ± 3.5	2.13 ± 0.17	25	20	1
	10 h 1200 °C	86.8 ± 8.3	1.20 ± 0.09	71	69	4
	100 h 1200 °C	97.7 ± 8.6	1.21 ± 0.06	78	80	4
	55 h 1400 °C	152.4 ± 19.5	1.12 ± 0.13	126	135	3
	10 h 1600 °C	164.5 ± 21.9	1.01 ± 0.08	147	159	4
	100 h 1600 °C	–	–	–	–	–
90:10:0	as sprayed	55.9 ± 4.1	1.90 ± 0.12	35	25	1
	10 h 1200 °C	127.1 ± 10.2	0.90 ± 0.11	122	135	3
	100 h 1200 °C	115.0 ± 20.0	0.72 ± 0.06	142	159	3
	55 h 1400 °C	101.6 ± 8.8	0.54 ± 0.07	175	195	3
	10 h 1600 °C	73.3 ± 12.3	0.43 ± 0.03	144	165	3
	100 h 1600 °C	44.7 ± 7.5	0.33 ± 0.06	135	123	4
90:5:5	as sprayed	54.8 ± 4.3	1.92 ± 0.15	30	25	1
	10 h 1200 °C	130.9 ± 13.0	0.97 ± 0.09	125	135	3
	100 h 1200 °C	146.9 ± 12.4	0.86 ± 0.10	145	170	3
	55 h 1400 °C	40.4 ± 3.8	0.54 ± 0.04	82	55	4
	10 h 1600 °C	19.5 ± 2.5	0.26 ± 0.12	63	30	4
	100 h 1600 °C	–	–	–	–	–
85:5:10	as sprayed	59.6 ± 6.3	1.84 ± 0.14	35	31	1
	10 h 1200 °C	145.7 ± 7.8	1.19 ± 0.10	113	123	4
	100 h 1200 °C	152.7 ± 8.5	1.04 ± 0.09	123	141	4
	55 h 1400 °C	32.9 ± 4.4	0.56 ± 0.11	90	30	4
	10 h 1600 °C	–	–	–	–	–
	100 h 1600 °C	–	–	–	–	–
85:10:5	as sprayed	58.5 ± 4.2	2.00 ± 0.14	33	28	1
	10 h 1200 °C	161.9 ± 13.1	1.06 ± 0.09	135	151	2–3
	100 h 1200 °C	145.9 ± 12.2	0.82 ± 0.06	150	172	3
	55 h 1400 °C	19.0 ± 1.1	1.37 ± 0.27	26	6	4
	10 h 1600 °C	56.4 ± 4.5	0.41 ± 0.06	105	125	4
	100 h 1600 °C	48.4 ± 6.1	0.36 ± 0.08	135	122	4
80:10:10	as sprayed	51.7 ± 3.5	1.80 ± 0.18	30	25	1
	10 h 1200 °C	140.7 ± 9.6	1.06 ± 0.11	120	130	3
	100 h 1200 °C	145.9 ± 16.4	0.82 ± 0.09	152	175	4
	55 h 1400 °C	17.4 ± 1.6	1.20 ± 0.46	23	6	4
	10 h 1600 °C	–	–	–	–	–
	100 h 1600 °C	–	–	–	–	–

The sintering activity that depends on the diffusion of the different atomic species determines the velocity of this process. The Ti^{4+} is much more mobile than Al^{3+} or Zr^{4+}, thus in titania containing composites the sintering effects start to change the mechanical properties much faster and at lower temperatures (Figs. 2–4). Surface diffusion is the important mechanism that determines the change of properties during heat treatment [64]. The second process of precipitating phases like tetragonal or monoclinic zirconia or zirconiumtitanate has a more complex influence on the mechanical properties. This can be best seen by comparing the compositions 100:0:0 with 90:0:10. Fig. 5 shows the measured bending strength as a function of the content of monoclinic zirconia for 90:0:10. The values of pure alumina at identical heat treatment level are added to separate this effect from the influence of the sintering process. From a certain monoclinic content there is a strong increase in bending strength due to particle and/or micro crack and/or transformation toughening mechanisms. If the monoclinic content becomes to high, the strength is decreased to zero. A similar effect causes the drop in strength in the ternary compositions. The velocity of this transformation is strongly increased by the presence of titania and some of the zirconia is bound in the form of zirconiumtitanate that lessens the detrimental effect of transformation into monoclinic zirconia.

3.2. Young's modulus

The Young's modulus in general follows the trend of the bending strength in the as sprayed as well as in the heat treated samples. Nonetheless it shows a non-linear behavior so that the

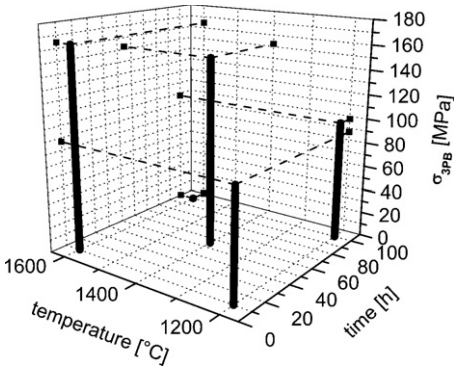

Fig. 3. Strength evolution of 90:0:10.

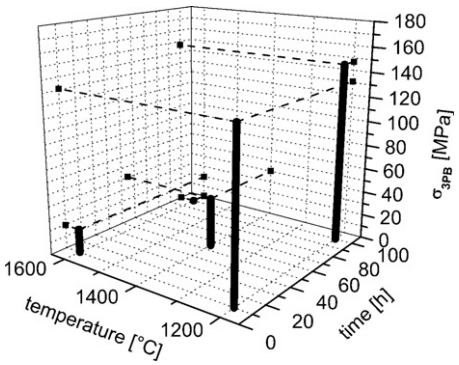

Fig. 4. Strength evolution of 90:5:5.

definition of a single number seems not appropriate. Thus the instantaneous modulus of the samples is displayed and discussed. For this the mathematical derivation of the stress–strain curve for each single measurement was calculated, the fracture strain standardized to equal 1 and than all curves were averaged. The values given in Table 4 for the Young's moduli are taken from this averaged curves; to indicate the non-linearity the value at 0.2 and 0.8 relative strain are shown. By looking at the individual instantaneous moduli four basic types can be distinct. Type one shows a more or less strong constant decrease and is representative for the as sprayed state. Two examples are shown in Figs. 6 and 7 representing the minimum (100:0:0) and the maximum (90:10:0) decrease of all tested

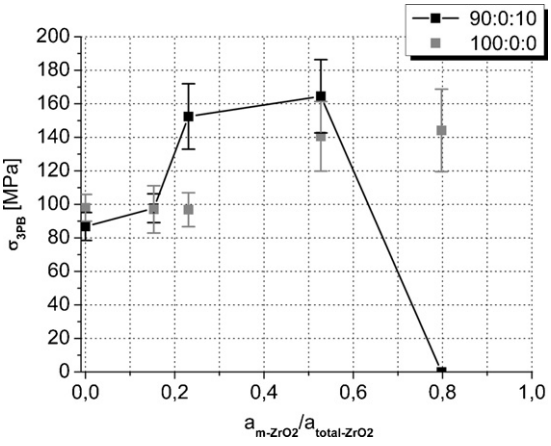

Fig. 5. Strength as a function of monoclinic zirconia content.

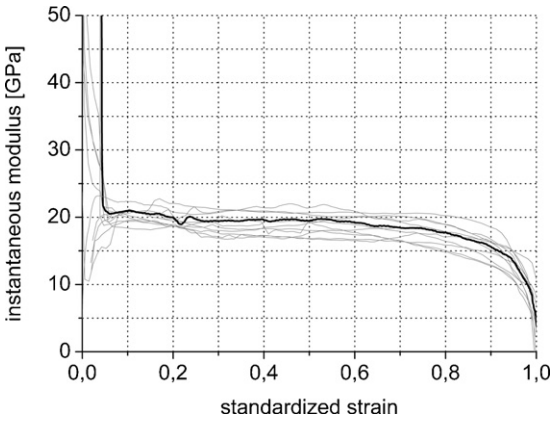

Fig. 6. Instantaneous modulus of 100:0:0 as sprayed (type 1).

compositions. After the first heat treatment stage this constant decrease changes into a plateau-like (type 2, Fig. 8) or constantly increasing type (type 3, Fig. 9). With longer temperature exposure a curved shape with a maximum develops (type 4, Fig. 10). In contrast to type 1–3 there is no such abrupt drop in the vicinity to a strain of 1. In general the decrease can be explained with growth of cracks leading to a softening of the sample. The increase might be explained with crack closure and increasing interlocking of the micro structural features. In type 4 this two mechanisms appear after each other leading to the maximum in the curve. The difference between the composi-

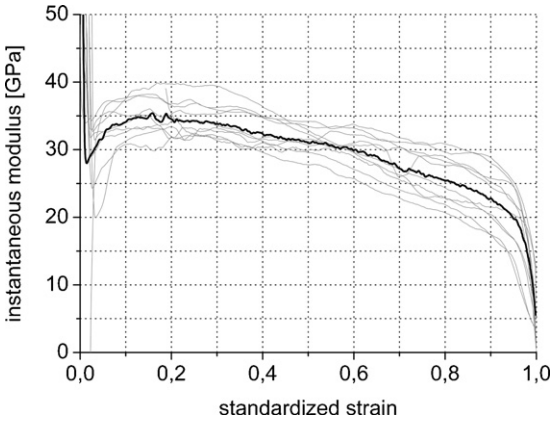

Fig. 7. Instantaneous modulus of 90:10:0 as sprayed (type 1).

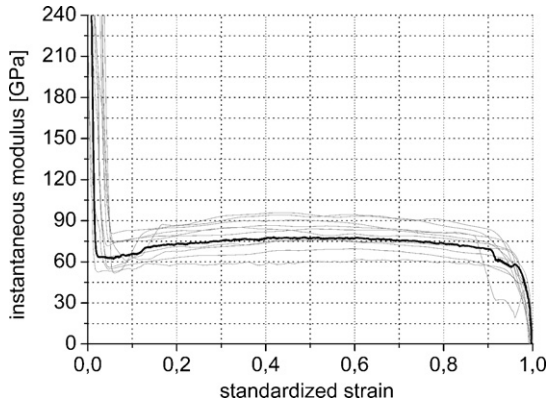

Fig. 8. Instantaneous modulus of 100:0:0 10 h 1200 °C (type 2).

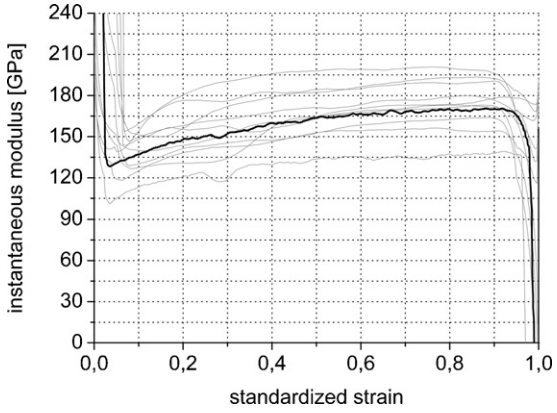

Fig. 9. Instantaneous modulus of 100:0:0 100 h 1600 °C (type 3).

tions lie in the speed they arrive at type 4. 90:0:10 and 85:5:10 reach type 4 already after the first treatment stage, 100:0:0 does not show type 4 behavior. A behavior similar to the here defined type 4 was observed by the authors of Ref. [65] in the as sprayed state and attributed to increasing splat interlocking followed by crack initiation during the experiment.

3.3. Thermal shock performance

To the best of the authors knowledge there are no published attempts of testing very thin free standing specimens in thermal shock experiments. That kind of test setup seems pointless at first view. At second view, by taking the width of the specimen and the applied method of water quenching into account it becomes clear, why significant changes in strength at certain temperature difference can occur. When the hot sample dips into the water, the part of the sample having contact with water cools down and shrinks. This causes stress in the sample. The already cooled part of the sample is under tensile, the neighboring hot part under compressive stress. This wave of tensile followed by compressive stress goes through the whole sample parallel to the immersion process. The magnitude of the strain is determined by the length of the isothermes, in case of vertical immersion this length is equal to the width of the sample. The thermal inertia is hereby very low due to very low total sample volume first reducing boiling effects and second guaranteeing immediate

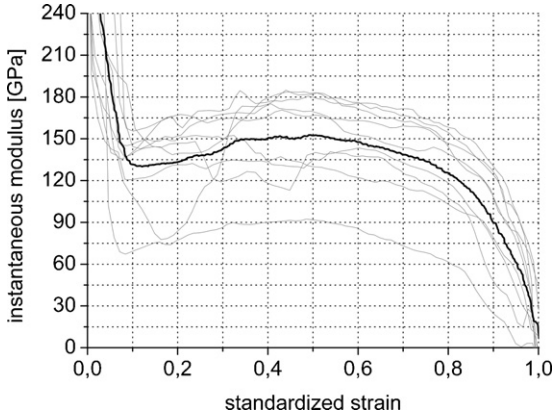

Fig. 10. Instantaneous modulus of 85:10:5 100 h 1600 °C (type 4).

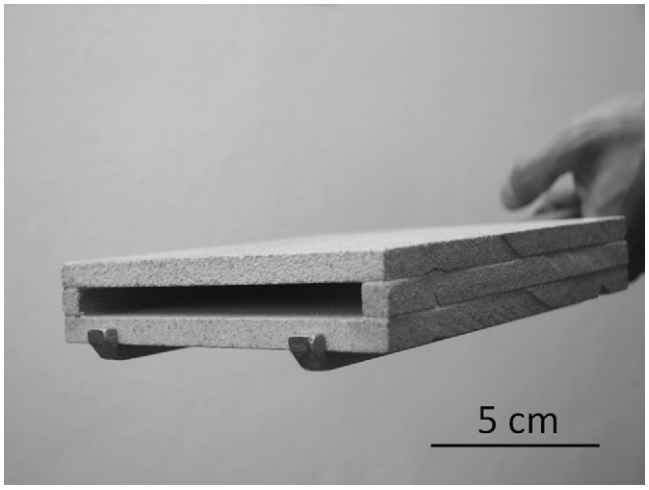

Fig. 11. Removable muffle.

temperature equalization between the sample and the cooling medium. The strain status can be assumed as planar. Four compositions were chosen for thermal shock experiments. To minimize sintering and phase change effects during heating up the samples in the thermal shock experiments all samples were previously annealed for 10 h at 1200 °C. 600 and 1000 K were chosen as ΔT for thermal shock. To minimize heat loss by radiation between removing the samples from the furnace and their contact with water a removable muffle (Fig. 11) was used. The muffle also guarantees a vertical immersion of the samples. There is significant loss in strength (Fig. 12) for samples shocked with $\Delta T = 600$ K except for 90:0:10. The higher starting strength level of 90:10:0 and 90:5:5 is caused by the increased sintering by the presence of titania. Compared to pure alumina the addition of only titania is detrimental and the addition of zirconia or zirconia plus titania beneficial for the remaining strength. After a shock with $\Delta T = 1000$ all compositions resemble at a low strength value between 10 and 15 MPa. This remaining strength might represent the contribution of the interlocking and pull-out mechanism to the complex strength in thermally sprayed materials. There seems no correlation between the type of instantaneous moduli and the loss of strength in the here tested compositions and treatment levels.

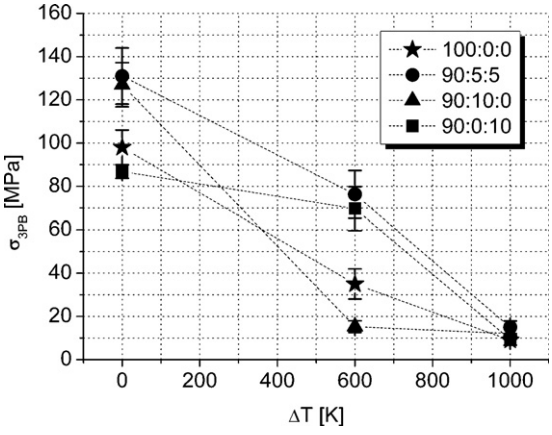

Fig. 12. Thermal shock behavior.

4. Conclusion

The here presented method of sample preparation and testing thin freestanding stripes leads to results that are comparable with published values in terms of absolute value and standard deviation. In the as sprayed state the addition of titania and zirconia to alumina increases the strength until a addition level of 15 wt%. After heat treatment the sintering causes strong increase in strength. The precipitation of second phases can influence the strength in both directions. For zirconia containing mixtures there is a critical value of the amount of monoclinic zirconia that leads to a complete loss in cohesion. The Young's moduli show distinct non-linear behavior. The increase is attributed to micro crack closure and increasing interlocking of the micro structural features and the decrease is caused by crack growth and crack recombination. It is possible to gain useful results from thermo shock experiments with thin specimens. The amount of stress is hereby determined by the width of the sample. The thermal shock resistance of thermally sprayed and annealed pure alumina is decreased by titania and increased by zirconia or zirconia plus titania additions.

References

[1] J. Suffner, H. Sieger, H. Hahn, S. Dosta, I.G. Cano, J.M. Guilemany, P. Klimczyk, L. Jaworska, Microstructure and mechanical properties of near-eutectic ZrO_2-60 wt.% Al_2O_3 produced by quenched plasma spraying, Materials Science and Engineering A 506 (2009) 180–186.

[2] F. Cernuschi, P.G. Bison, S. Marinetti, P. Scardi, Thermophysical, mechanical and microstructural characterization of aged free-standing plasma-sprayed zirconia coatings, Acta Materialia 56 (2008) 4477–4488.

[3] B. Ercan, K.J. Bowman, R.W. Trice, H. Wang, W. Porter, Effect of initial powder morphology on thermal and mechanical properties of stand-alone plasma-sprayed 7 wt.% Y_2O_3–ZrO_2 coatings, Materials Science and Engineering A 435–436 (2006) 212–220.

[4] T. Hilpert, E. Ivers-Tiffée, Correlation of electrical and mechanical properties of zirconia based thermal barrier coatings, Solid State Ionics 175 (2004) 471–476.

[5] S.R. Choi, D. Zhu, R.A. Miller, Mechanical properties/database of plasma-sprayed ZrO_2-8wt% Y_2O_3 thermal barrier coatings, The International Journal of Applied Ceramic Technology 1 (2004) 330–342.

[6] P. Bansal, N.P. Padture, A. Vasiliev, Improved interfacial mechanical properties of Al_2O_3-13wt%TiO_2 plasma-sprayed coatings derived from nanocrystalline powders, Acta Materialia 51 (2003) 2959–2970.

[7] H.-J. Kim, C.-H. Lee, Y.-G. Kweon, The effects of sealing on the mechanical properties of the plasma-sprayed alumina–titania coating, Surface and Coatings Technology 139 (2001) 75–80.

[8] R.J. Damani, D. Rubesa, R. Danzer, Fracture toughness, strength and thermal shock behaviour of bulk plasma sprayed alumina – effects of heat treatment, Journal of the European Ceramic Society 20 (2000) 1439–1452.

[9] R.J. Damani, A. Wanner, Microstructure and elastic properties of plasma-sprayed alumina, Journal of Materials Science 35 (2000) 4307–4318.

[10] E. Rigal, T. Priem, E. Vray, Mechanical properties of as-sprayed and annealed partially stabilized zirconia, in: A. Ohmori (Ed.), ITSC 95 Kobe: High Temperature Society of Japan, Osaka, Japan, 1995.

[11] E.H. Lutz, Microstructure and properties of plasma ceramics, Journal of the American Ceramic Society 77 (1994) 1274–1280.

[12] W.Z. Li, Y. Yao, Y.Q. Li, J.B. Li, J. Gong, C. Sun, X. Jiang, Damage behavior of the NiCrAlY coating systems with or without barrier layer during three-point bending, Materials Science and Engineering A 512 (2009) 117–125.

[13] Y. Liu, T. Nakamura, G. Dwivedi, A. Valarezo, S. Sampath, Anelastic behavior of plasma-sprayed zirconia coatings, Journal of the American Ceramic Society 91 (2008) 4036–4043.

[14] A.D. Jadhav, N.P. Padture, Mechanical properties of solution-precursor plasma-sprayed thermal barrier coatings, Surface and Coatings Technology 202 (2008) 4976–4979.

[15] M. Gaona, R.S. Lima, B.R. Marple, Influence of particle temperature and velocity on the microstructure and mechanical behaviour of high velocity oxy-fuel (HVOF)-sprayed nanostructured titania coatings, Journal of Materials Processing Technology 198 (2008) 426–435.

[16] Y. Wang, W. Tian, Y. Yang, Thermal shock behavior of nanostructured and conventional Al_2O_3/13 wt%TiO_2 coatings fabricated by plasma spraying, Surface and Coatings Technology 201 (2007) 7746–7754.

[17] R.S. Lima, B.R. Marple, From APS to HVOF spraying of conventional and nanostructured titania feedstock powders: a study on the enhancement of the mechanical properties, Surface and Coatings Technology 200 (2006) 3428–3437.

[18] P.L. Ke, Q.M. Wang, J. Gong, C. Sun, Y.C. Zhou, Progressive damage during thermal shock cycling of D-gun sprayed thermal barrier coatings with hollow spherical ZrO_2–$8Y_2O_3$, Materials Science and Engineering A 435–436 (2006) 228–236.

[19] E. Celik, O. Culha, B. Uyulgan, N.F. Ak Azem, I. Ozdemir, A. Turk, Assessment of microstructural and mechanical properties of HVOF sprayed WC-based cermet coatings for a roller cylinder, Surface and Coatings Technology 200 (2006) 4320–4328.

[20] A.F.M. Arif, B.S. Yilbas, Three-point bend testing of HVOF Inconel 625 coating: FEM simulation and experimental investigation, Surface and Coatings Technology 201 (2006) 1873–1879.

[21] C.-S. Zhai, J. Wang, F. Li, J.-C. Tao, Y. Yang, B.-D. Sun, Thermal shock properties and failure mechanism of plasma sprayed Al_2O_3/TiO_2 nanocomposite coatings, Ceramics International 31 (2005) 817–824.

[22] B.S. Yilbas, A.F.M. Arif, M.A. Gondal, HVOF coating and laser treatment: three-point bending tests, Journal of Materials Processing Technology 164–165 (2005) 954–957.

[23] S.C. Okumus, Microstructural and mechanical characterization of plasma sprayed Al_2O_3–TiO_2 composite ceramic coating on Mo/cast iron substrates, Materials Letters 59 (2005) 3214–3220.

[24] A.M. Limarga, S. Widjaja, T.H. Yip, Mechanical properties and oxidation resistance of plasma-sprayed multilayered Al_2O_3/ZrO_2 thermal barrier coatings, Surface and Coatings Technology 197 (2005) 93–102.

[25] X. Lin, Y. Zeng, S.W. Lee, C. Ding, Characterization of alumina-3 wt.% titania coating prepared by plasma spraying of nanostructured powders, Journal of the European Ceramic Society 24 (2004) 627–634.

[26] C.-J. Li, W.-Z. Wang, Y. He, Measurement of fracture toughness of plasma-sprayed Al_2O_3 coatings using a tapered double cantilever beam method, Journal of the American Ceramic Society 86 (2003) 1437–1439.

[27] E.H. Jordan, M. Gell, Y.H. Sohn, D. Goberman, L. Shaw, S. Jiang, M. Wang, T.D. Xiao, Y. Wang, P. Strutt, Fabrication and evaluation of plasma sprayed nanostructured alumina–titania coatings with superior properties, Materials Science and Engineering A 301 (2001) 80–89.

[28] S.W.K. Kweh, K.A. Khor, P. Cheang, Plasma-sprayed hydroxyapatite (HA) coatings with flame-spheroidized feedstock: microstructure and mechanical properties, Biomaterials 21 (2000) 1223–1234.

[29] A. Kucuk, C.C. Berndt, U. Senturk, R.S. Lima, C.R.C. Lima, Influence of plasma spray parameters on mechanical properties of yttria stabilized zirconia coatings. I: four point bend test, Materials Science and Engineering A 284 (2000) 29–40.

[30] K.A. Khor, Z.L. Dong, Y.W. Gu, Influence of oxide mixtures on mechanical properties of plasma sprayed functionally graded coating, Thin Solid Films 368 (2000) 86–92.

[31] J.D. Haman, K.K. Chittur, D.E. Crawmer, L.C. Lucas, Analytical and mechanical testing of high velocity oxy-fuel thermal sprayed and plasma sprayed calcium phosphate coatings, Journal of Biomedical Materials Research 48 (1999) 856–860.

[32] Y.C. Tsui, C. Doyle, T.W. Clyne, Plasma sprayed hydroxyapatite coatings on titanium substrates. Part 1: mechanical properties and residual stress levels, Biomaterials 19 (1998) 2015–2029.

[33] D. Schwingel, R. Taylor, T. Haubold, J. Wigren, C. Gualco, Mechanical and thermophysical properties of thick PYSZ thermal barrier coatings: correlation with microstructure and spraying parameters, Surface and Coatings Technology 108–109 (1998) 99–106.
[34] O. Brandt, Mechanical properties of HVOF coatings, Journal of Thermal Spray Technology 4 (1995) 147–152.
[35] D. Zois, A. Lekatou, M. Vardavoulias, A microstructure and mechanical property investigation on thermally sprayed nanostructured ceramic coatings before and after a sintering treatment, Surface and Coatings Technology 204 (2009) 15–27.
[36] Y. Wang, H. Guo, S. Gong, Thermal shock resistance and mechanical properties of $La_2Ce_2O_7$ thermal barrier coatings with segmented structure, Ceramics International 35 (2009) 2639–2644.
[37] S.-I. Jung, J.-H. Kim, J.-H. Lee, Y.-G. Jung, U. Paik, K.-S. Lee, Microstructure and mechanical properties of zirconia-based thermal barrier coatings with starting powder morphology, Surface and Coatings Technology 204 (2009) 802–806.
[38] Z. Yin, S. Tao, X. Zhou, C. Ding, Particle in-flight behavior and its influence on the microstructure and mechanical properties of plasma-sprayed Al_2O_3 coatings, Journal of the European Ceramic Society 28 (2008) 1143–1148.
[39] J. Oberste Berghaus, J.-G. Legoux, C. Moreau, F. Tarasi, T. Chráska, Mechanical and thermal transport properties of suspension thermal-sprayed alumina–zirconia composite coatings, Journal of Thermal Spray Technology 17 (2008) 91–104.
[40] O. Culha, E. Celik, N.F. Ak Azem, I. Birlik, M. Toparli, A. Turk, Microstructural, thermal and mechanical properties of HVOF sprayed Ni–Al-based bond coatings on stainless steel substrate, Journal of Materials Processing Technology 204 (2008) 221–230.
[41] R. Yilmaz, A.O. Kurt, A. Demir, Z. TatlI, Effects of TiO_2 on the mechanical properties of the Al_2O_3-TiO_2 plasma sprayed coating, Journal of the European Ceramic Society 27 (2007) 1319–1323.
[42] A. Ibrahim, R.S. Lima, C.C. Berndt, B.R. Marple, Fatigue and mechanical properties of nanostructured and conventional titania (TiO_2) thermal spray coatings, Surface and Coatings Technology 201 (2007) 7589–7596.
[43] R. Venkataraman, R. Krishnamurthy, Evaluation of fracture toughness of as plasma sprayed alumina-13 wt.% titania coatings by micro-indentation techniques, Journal of the European Ceramic Society 26 (2006) 3075–3081.
[44] K.A. Habib, J.J. Saura, C. Ferrer, M.S. Damra, E. Giménez, L. Cabedo, Comparison of flame sprayed Al_2O_3/TiO_2 coatings: their microstructure, mechanical properties and tribology behavior, Surface and Coatings Technology 201 (2006) 1436–1443.
[45] P. Ctibor, P. Bohác, M. Stranyánek, R. Ctvrtlík, Structure and mechanical properties of plasma sprayed coatings of titania and alumina, Journal of the European Ceramic Society 26 (2006) 3509–3514.
[46] G. Antou, G. Montavon, F. Hlawka, C. Coddet, A. Cornet, Structural evolution and mechanical properties modification of MELTPRO (in situ remelted) processed thermal barrier coatings during thermal shocks, Advanced Engineering Materials 8 (2006) 657–663.
[47] G. Bolelli, V. Cannillo, L. Lusvarghi, T. Manfredini, C. Siligardi, C. Bartuli, A. Loreto, T. Valente, Plasma-sprayed glass-ceramic coatings on ceramic tiles: microstructure, chemical resistance and mechanical properties, Journal of the European Ceramic Society 25 (2005) 1835–1853.
[48] Y. Qiao, T.E. Fischer, A. Dent, The effects of fuel chemistry and feedstock powder structure on the mechanical and tribological properties of HVOF thermal-sprayed WC-Co coatings with very fine structures, Surface and Coatings Technology 172 (2003) 24–41.
[49] Y. Liu, T.E. Fischer, A. Dent, Comparison of HVOF and plasma-sprayed alumina/titania coatings – microstructure, mechanical properties and abrasion behavior, Surface and Coatings Technology 167 (2003) 68–76.
[50] Y. Li, K.A. Khor, Mechanical properties of the plasma-sprayed Al_2O_3/$ZrSiO_4$ coatings, Surface and Coatings Technology 150 (2002) 143–150.
[51] L.L. Shaw, D. Goberman, R. Ren, M. Gell, S. Jiang, Y. Wang, T.D. Xiao, P.R. Strutt, The dependency of microstructure and properties of nanostructured coatings on plasma spray conditions, Surface and Coatings Technology 130 (2000) 1–8.
[52] S. Ahmaniemi, P. Vuoristo, T. Mäntylä, Mechanical and elastic properties of modified thick thermal barrier coatings, Materials Science and Engineering A 366 (2004) 175–182.
[53] P.A. Langjahr, R. Oberacker, M.J. Hoffmann, Long-term behavior and application limits of plasma-sprayed zirconia thermal barrier coatings, Journal of the American Ceramic Society 84 (2001) 1301–1308.
[54] H.-J. Kim, Y.-G. Kweon, Elastic modulus of plasma-sprayed coatings determined by indentation and bend tests, Thin Solid Films 342 (1999) 201–206.
[55] C.A. Johnson, J.A. Ruud, A.C. Kaya, H.G. De Lorenzi, A method for measuring non-linear elastic properties of thermal barrier coatings, in: C.C. Berndt, S. Sampath (Eds.), Advances in Thermal Spray Science and Technology, Proceedings of the 8th National Thermal Spray Conference, Materials Park, Ohio, ASM International, Houston, 1995, pp. 415–420.
[56] I. Sevostianov, M. Kachanov, Plasma-sprayed ceramic coatings: anisotropic elastic and conductive properties in relation to the microstructure; cross-property correlations, Materials Science and Engineering A 297 (2001) 235–243.
[57] N.N. Ault, C. Norton, Characteristics of refractory oxide coatings produced by flame-spraying, Journal of the American Ceramic Society 40 (1957) 69–74.
[58] M. Arai, M. Furuse, Evaluating strength of thermally sprayed Al_2O_3 on aluminum, Vacuum 84 (2009) 672–676.
[59] M. Sasaki, M. Nakagawa, T. Miyazaki, R. Urao, Adhesion of plasma sprayed alumina–titania layer at high temperatures. Surface Modification Technologies XI, in: T.S. Sudarshan, M. Jeandin, K.A. Khor (Eds.), Proceedings of the 11th International Conference on Surface Modification Technologies, London, UK, Institute of Materials, Paris, 1997, pp. 137–147.
[60] C.G. Aneziris, P. Gehre, T. Kratschmer, H. Berek, Thermal shock behavior of flame-sprayed free-standing coatings based on Al_2O_3 with TiO_2- and ZrO_2-additions, International Journal of Applied Ceramic Technology, in press, doi:10.1111/j.1744-7402.2010.02535.x.
[61] T. Kratschmer, Flammgespritzte Schichten im System Al_2O_3–TiO_2–ZrO_2. Dissertation. Freiberg, 2010.
[62] T. Kratschmer, P. Gehre, C.G. Aneziris, Flame spraying of alumina with titania and zircinia additions, in: P. Quirmbach (Ed.), 51st International Colloquium on Refractories, vol. 51, Bonn, Germany, Forschungsgemeinschaft Feuerfest e.V., Aachen, 2008, pp. 24–27.
[63] T. Kratschmer, C.G. Aneziris, Amorphous zones in flame sprayed alumina–titania–zirconia compounds, Ceramics International 37 (2011) 181–188.
[64] A. Cipitria, I.O. Golosnoy, T.W. Clyne, A sintering model for plasma-sprayed zirconia TBCs. Part I: free-standing coatings, Acta Materialia 57 (2009) 980–992.
[65] F. Tang, J.M. Schoenung, Evolution of Young's modulus of air plasma sprayed yttria-stabilized zirconia in thermally cycled thermal barrier coatings, Scripta Materialia 54 (2006) 1587–1592.